Hindawi
International Journal of Photoenergy
Volume 2020, Article ID 4065359, 9 pages
https://doi.org/10.1155/2020/4065359

Research Article

An Ignored Wind Generates More Electricity: A Solar Updraft Tower to a Wind Solar Tower

Koichi Watanabe,[1] **Sho Fukutomi**,[2] **Yuji Ohya**,[3] **and Takanori Uchida**[3]

[1]*Kyushu University Platform of Inter/Transdisciplinary Energy Research (Q-PIT), Kyushu University, Kasuga 816-8580, Japan*
[2]*Department of Aeronautics and Astronautics, Kyushu University, Fukuoka 819-0395, Japan*
[3]*Research Institute for Applied Mechanics, Kyushu University, Kasuga 816-8580, Japan*

Correspondence should be addressed to Koichi Watanabe; koichi-watanabe@riam.kyushu-u.ac.jp

Received 19 October 2019; Accepted 7 February 2020; Published 11 March 2020

Guest Editor: Ting-Zhen Ming

A solar updraft tower is one of the wind power generation plants which utilizes solar energy. The purpose of this study was to ascertain whether the tower was also able to utilize crosswind energy. Wind tunnel experiments and numerical simulations were conducted simulating the crosswind. The results showed that suctioned updraft speed in the tower was proportional to the crosswind speed, and its conversion rate depended on the tower configuration. A diffuser-shaped tower with a vortex generator achieved to produce the updraft whose speed exceeded the crosswind speed. It was due to the low pressure created by the vortex atop the tower and to the diffuser effect. The crosswind utilization enables the simple power generation device to generate electricity during the night, and the hybrid utilization of renewable energies contributes to the increasing wind energy market.

1. Introduction

A solar updraft tower is one of the renewable energy power plants. The tower originally utilizes solar energy alone; thus, it does not work during the night. The purpose of this study was to ascertain whether the tower was also able to utilize crosswind energy. The hybrid utilization concept of renewable energies was expected to contribute to the increasing wind energy market due to its time independency of power generation and relatively high input energy density.

A traditional solar updraft tower has three essential components—a transparent roof collector, a cylindrical hollow tower, and a wind turbine with an electricity generator. Hot air is produced in the collector by solar radiation to the ground. The air loses weight due to its thermal expansion and is drawn upward inside the tower by buoyancy (see Figure 1(a)). The thermal updraft drives the turbine installed at the base of the tower, and it produces electricity. The original concept of the solar updraft tower was validated by Haaf et al. [1, 2] in 1980s.

By contrast, power generations utilizing crosswind with a tower structure have never been popular, although there are few patents [3, 4]. Regarding the solar updraft tower, there are several researches concerning the effect of the crosswind. Pretorius and Kröger [5] simulated performance of the solar power plant and predicted that windy conditions would impair the performance. Ming et al. [6, 7] and Zou et al. [8] also perceived its negative effect and proposed some collector configurations to avoid it. However, Ming et al. [9, 10] pointed out that strong crosswind had the possibility of increasing the output power of the tower. Other numerical studies [11–13] have supported the suggestion.

This study attempted to enhance the positive effect of the crosswind. We investigated new approaches using a vortex generator and a diffuser-shaped tower in wind tunnel experiments and numerical simulations. The vortex generator was just a flat plate on the tower (see Figure 1(b)). Vortices generated by the plate lowered pressure atop the tower, and the low pressure created suctioned updraft in the tower. The suitability of the diffuser-shaped tower was already verified in

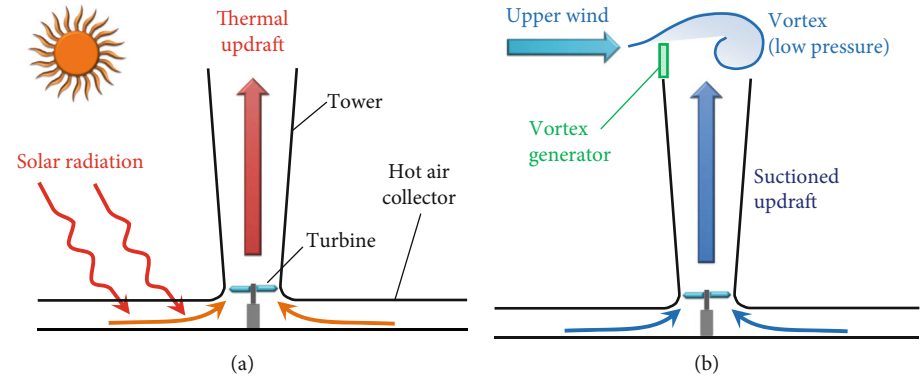

Figure 1: The mechanisms of the wind solar tower: (a) solar energy utilization of the WST; (b) wind energy utilization of the WST.

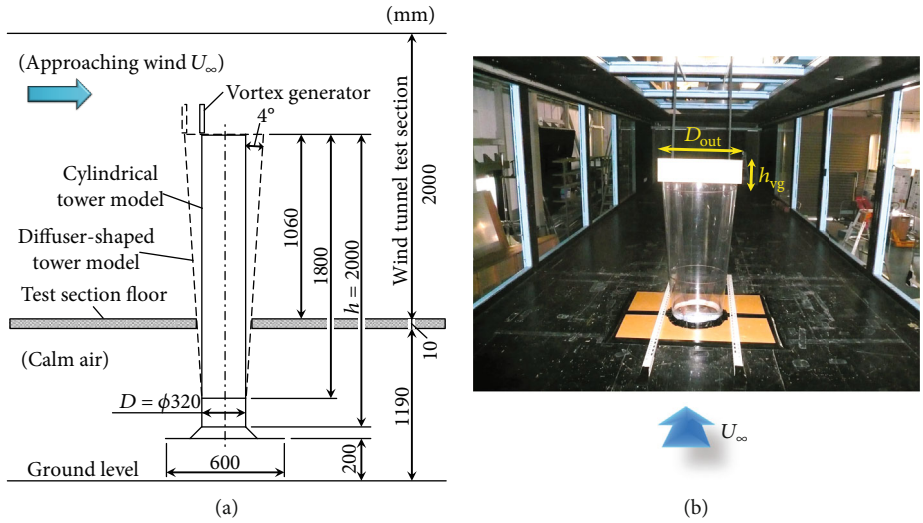

Figure 2: The tower model set-up in the wind tunnel experiments: (a) dimensions of the tower model and its set-up; (b) in situ photograph of the tower and the vortex generator in the wind tunnel.

our previous study using thermal updraft [14]. We have applied the similar mechanism in our brimmed-diffuser augmented wind turbines and achieved large output power increase [15–17]. Importantly, the new approach enabled the solar updraft tower to utilize two different renewable energies simultaneously, although such a hybrid approach is usually achieved by several devices in the same location [18, 19]. We call the tower "a wind solar tower" (WST) which has two mechanisms shown in Figure 1.

2. Materials and Methods

2.1. Wind Tunnel Experiments. We conducted wind tunnel experiments to verify the wind power utilization of the WST. The large boundary layer wind tunnel of the Research Institute for Applied Mechanics, Kyushu University, was used. The wind tunnel had a test section of 15 m long × 3.6 m wide × 2 m high, with a maximum wind velocity of 30 m/s, and was characterized by a low turbulence intensity of 0.4%. To minimize blockage effects, half of the test section's side walls and ceiling panels were removed.

In general, wind in the field is decelerated near the ground due to the shear stress on the ground. Therefore, the approaching crosswind speed has nonuniform distribution in the vertical direction. This means that the tower top has the stronger wind than the bottom does. We set our tower model through the test section floor of the wind tunnel in order to simulate such a situation. This method made it possible that wind approached only the upper side of the tower. Figure 2 shows the tower model and its set-up. We investigated a cylindrical tower and diffuser-shaped tower whose diameter D was 0.32 m and height h was 2.0 m. The height of the vortex generator h_{vg} was $D/2$ or D, and the width of the vortex generator was the same as the diameter of the tower outlet $D_{out} = D + 2h \cdot \tan \alpha$, where α was the semiopen angle of the tower. A wind turbine was not installed in any cases.

We measured updraft speed w and static pressure difference Δp_s from the pressure at the point in calm air. The wind speed was measured with a hot-wire anemometer and hot-sphere anemometers. The pressure difference was measured with a static tube and a digital manometer in the approaching

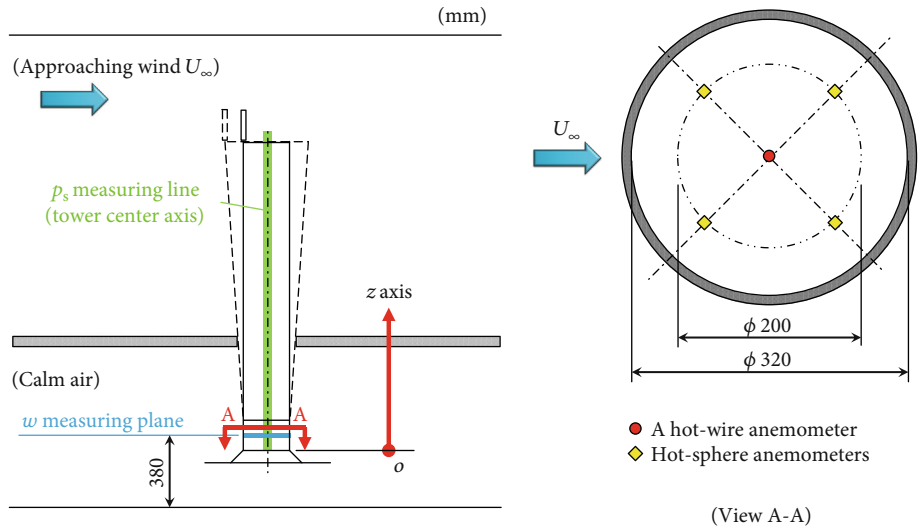

Figure 3: The measuring points of the updraft speed w and static pressure difference Δp_s.

Table 1: The conditions of the numerical simulation.

Conditions	
Simulation method	LES
SGS model	Wale
Convective term	Bounded central scheme
Time derivative term	1st-order implicit scheme

wind speed of 8 m/s. Figure 3 shows the measuring points. A smoke generator was used for the flow visualization in the approaching wind speed of 4 m/s.

We defined a pressure coefficient C_p by Equation (1). The value is derived from the static pressure difference divided by the dynamic pressure of the approaching wind.

$$C_p = \frac{\Delta p_s}{(1/2)\rho U_\infty{}^2}, \quad (1)$$

2.2. Numerical Simulations. A commercial fluid analysis software "STAR-CCM+" [20] was used for the numerical experiments. Table 1 shows the numerical conditions. Figure 4(a) shows the computational domain, and Figure 4(b) shows the computational grid. This computational domain was similar to the wind tunnel experiment; the domain had not only the upper section where wind blew but also the lower section where the air was calm. To minimize blockage effects, a larger domain in comparison of the tower diameter was created (Figure 4). The nonstructural grid pattern consisted mainly of decahedron. The approaching wind speed was set to 2, 4, 6, or 8 m/s. Nonslip boundary conditions were applied at the ground floor, the flow section floor, and the surface of the body. Slip boundary conditions were applied at the side and upper boundaries. The Neumann condition was given to pressures at the domain boundaries. The flow patterns with a cylindrical tower and a diffuser-shaped tower were simulated. The numerical tower models were the same to the experimental models in their configurations. We also conducted some simulations with the vortex generators. A wind turbine was not simulated in any cases.

3. Results and Discussion

3.1. Experimental Results. Figure 5 shows the updraft wind speeds w in the cylindrical towers. Measured values were plotted in the figure, and fit curves were applied with their equations. Obviously, the updraft wind speeds increased proportional to the approaching wind speed U_∞ in all cases. The cylindrical tower with the short vortex generator ($h_{vg} = D/2$) achieved 1.8 times increase in the updraft speed. However, enlarging the height of the vortex generator did not lead to significant increase of the speed unexpectedly. The tower with the tall vortex generator ($h_{vg} = D$) achieved 1.9 times increase in the updraft speed.

Figure 6 shows w in the diffuser-shaped towers. The updraft wind speeds increased proportional to the approaching wind speed. The diffuser-shaped tower without the vortex generator achieved 2.1 times increase in the updraft speed compared to the cylindrical tower. The diffuser-shaped tower with the short vortex generator ($h_{vg} = D/2$) achieved 1.3 times increase in the updraft speed, although enlarging the height of the vortex generator did not lead to significant increase of the speed. The tower with the tall vortex generator ($h_{vg} = D$) achieved 1.4 times increase in the updraft speed. The diffuser-shaped towers with the vortex generators created notable updraft whose speed exceeded the approaching wind speed.

Photos in Figure 7 show updraft visualization results by smoke in the wind tunnel. The crosswind flew left to right. In the case of the tower without the vortex generator (Figure 7(a)), the updraft immediately flew downstream at the tower outlet. As the height of the vortex generator became higher, the updraft suctioned up to the top of the vortex generators. At the separated shear layer, vortices were shed by its

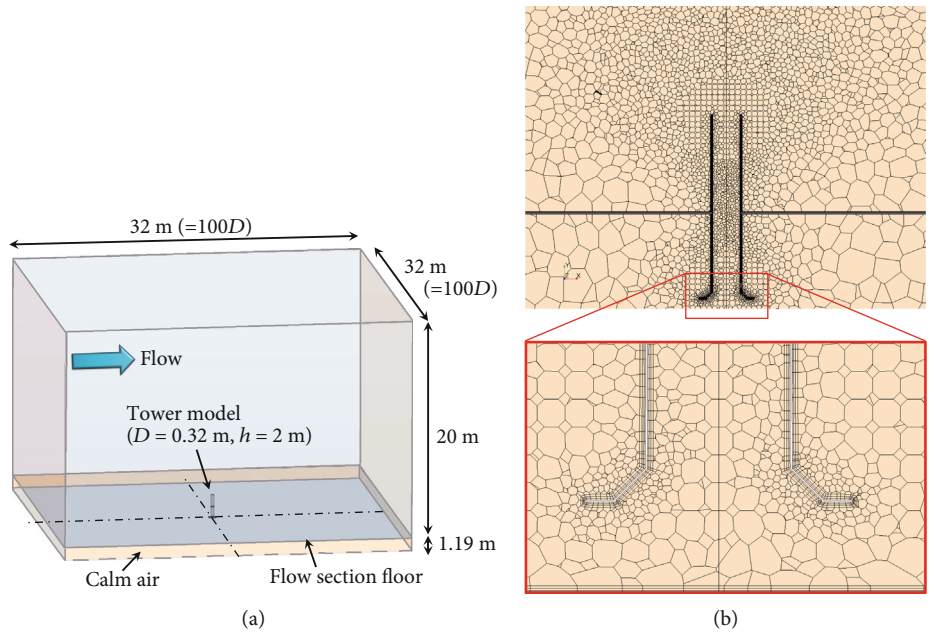

Figure 4: The numerical domain: (a) a schematic of the calculation domain; (b) the computational grid.

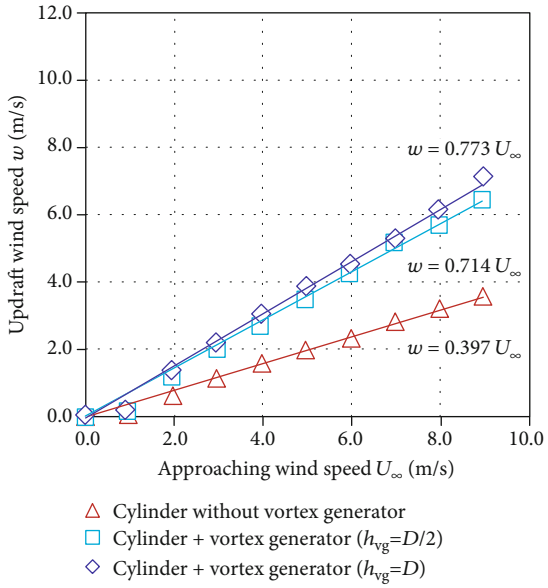

Figure 5: Updraft wind speeds in the case of the cylindrical tower (experimental results).

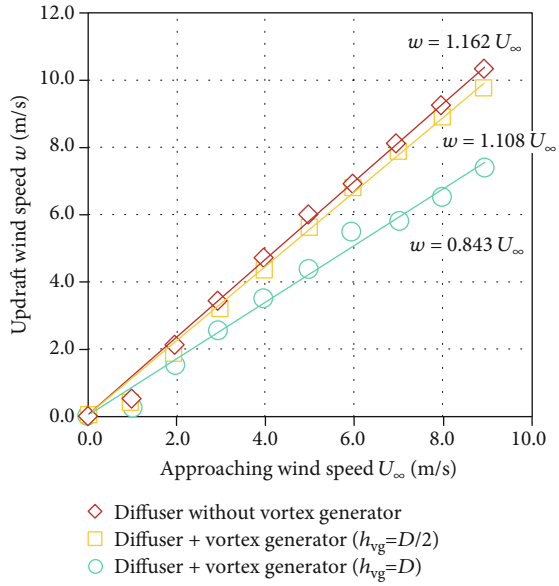

Figure 6: Updraft wind speeds in the case of the diffuser-shaped tower (experimental results).

shear stress. At the same time, large vortices were observed in each cases (Figures 7(d)–7(f)). The yellow arrows show the positions of the vortices. In the case of the tower without the vortex generator (Figure 7(d)), the vortex produced downstream of the tower. As the height of the vortex generator became higher, the vortex position moved upstream, that was, right above the tower outlet. However, the vortex position also moved upward. We assumed that the expansion of the distance between the vortex and the tower outlet prevented to enhance the updraft suctioning.

Figure 8 shows the pressure distributions measured in the experiments. In the cases of the diffuser-shaped tower, the pressure lowered near the tower inlet due to its diffuser effect. At the same time, the pressure wholly lowered in the cases with the vortex generators. Therefore, the diffuser-shaped tower with the vortex generator achieved the lowest pressure, and it lead to the highest updraft wind speed.

Here, we provide a simple theory in order to give some explanations to the experimental results. We defined

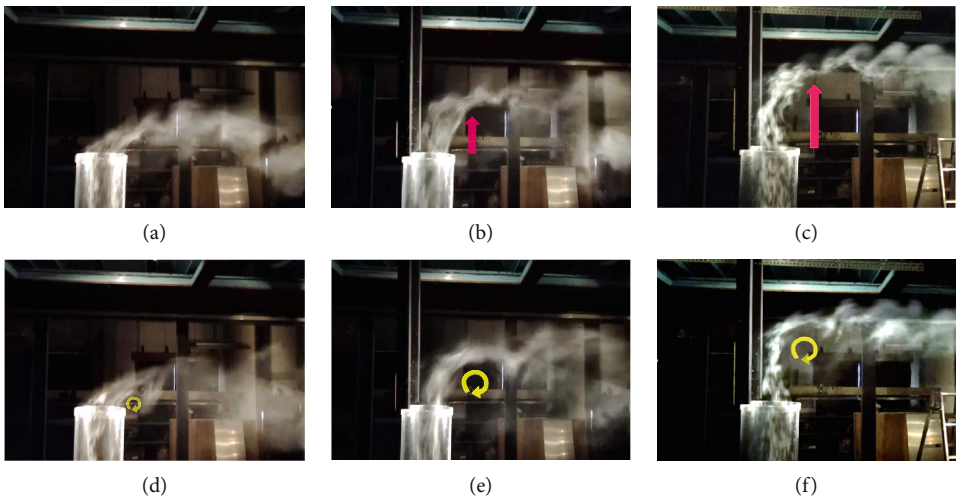

Figure 7: The updraft suctioned up to the top of the vortex generators and large vortices produced by the crosswind: (a) the cylindrical tower without the vortex generator; (b) the cylindrical tower with the vortex generator ($h_{vg} = D/2$); (c) the cylindrical tower with the vortex generator ($h_{vg} = D$); (d) the cylindrical tower without the vortex generator; (e) the cylindrical tower with the vortex generator ($h_{vg} = D/2$); (f) the cylindrical tower with the vortex generator ($h_{vg} = D$).

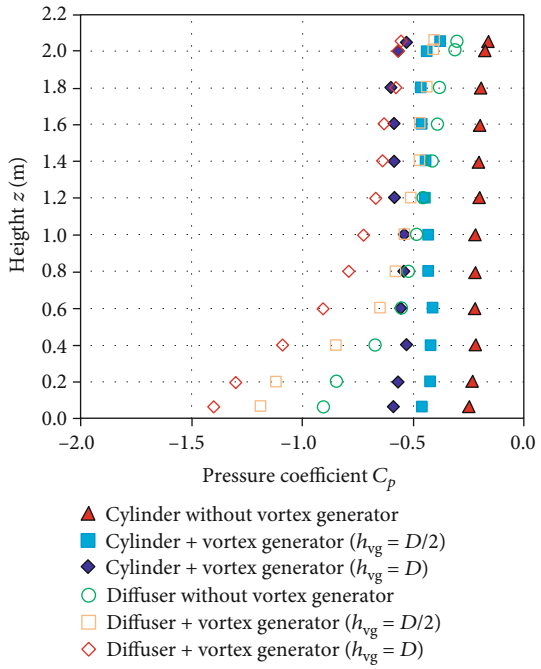

Figure 8: Pressure distributions in the towers (experimental results).

variables as shown in Figure 9. Considering mass conservation and pressure balance, we derived the following equation:

$$w_{thr} = \sqrt{\frac{C_{pb}}{\{\xi_{in} + \xi_{dif} + (1 + \xi_{out})(A_{thr}/A_{out})^2\}}} U_{\infty}, \quad (2)$$

where C_{pb} is the back pressure coefficient of the vortex generator ($\Delta p/(1/2)\rho {U_{\infty}}^2$), ξ_{in} is the pressure loss coefficient at the tower inlet, ξ_{dif} is the pressure loss coefficient in the diffuser, and ξ_{out} is the pressure loss coefficient at the tower outlet.

Equation (2) supports the experimental trend that the updraft wind speed is proportional to the crosswind speed.

3.2. Numerical Results. Figures 10 and 11 show the updraft wind speeds w derived by the numerical simulations. The simulated values were plotted in the figures with the plots and fit curves derived by the experiments. The numerical results showed good agreements with the experimental results.

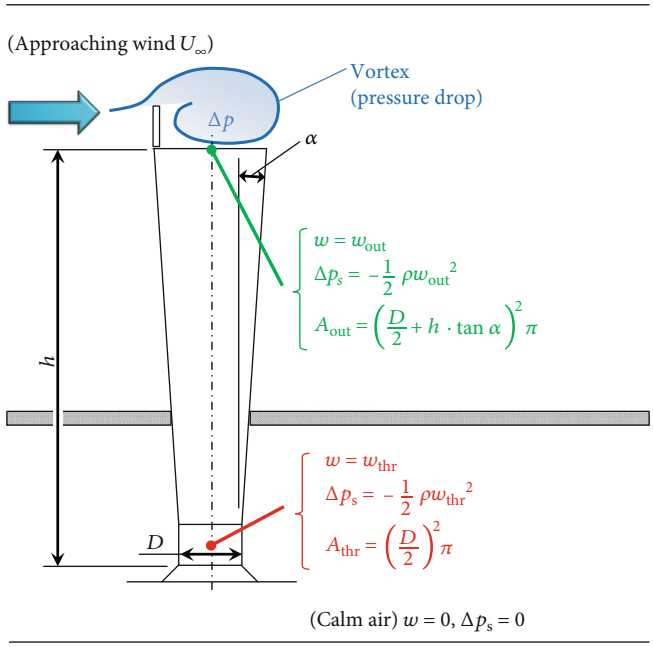

Figure 9: The schematic of the phenomenon around the WST.

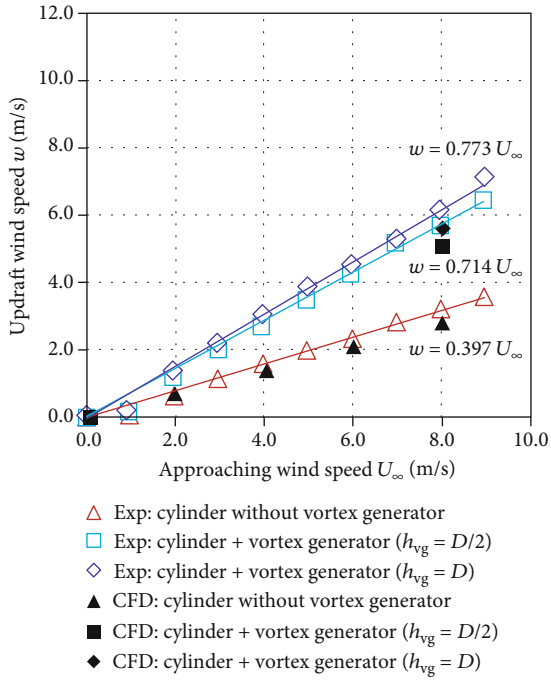

Figure 10: Updraft wind speeds in the case of the cylindrical tower. The solid symbols represent the numerical results. The open symbols represent the experimental results.

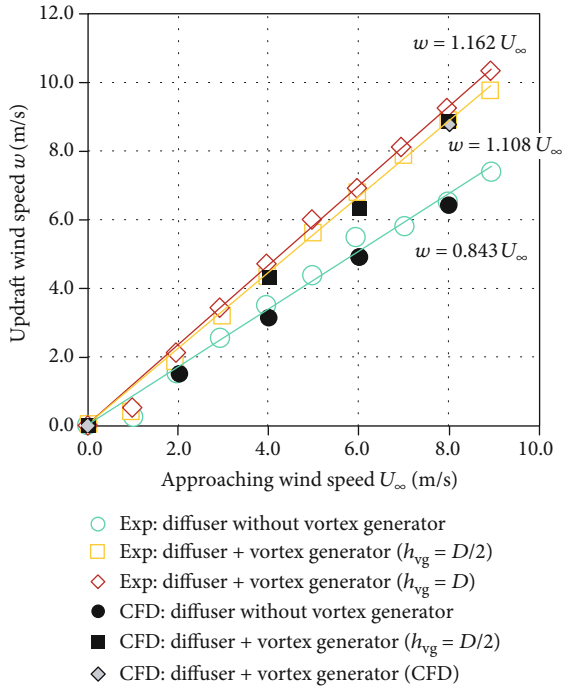

Figure 11: Updraft wind speeds in the case of the diffuser-shaped tower. The solid symbols represent the numerical results. The open symbols represent the experimental results.

Figure 12 shows pressure distributions in the towers derived by numerical simulations. The numerical results showed the same trend as the experimental results. Hence, we considered both our experimental results and numerical results were reliable.

Figure 13 shows time-averaged pressure distributions. One notable point was that there appeared some pressure drops above the towers. The pressure above the towers with the vortex generator lowered. They were due to the pressure lowness of vortices produced by the vortex generator.

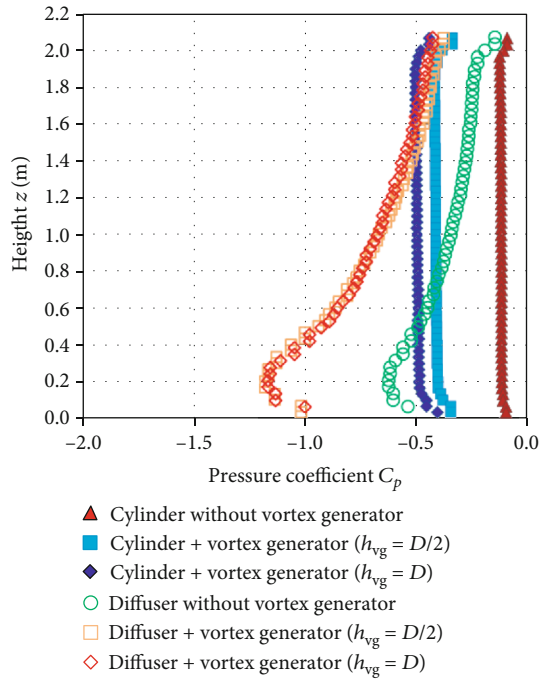

Figure 12: Pressure distributions in the towers (numerical results).

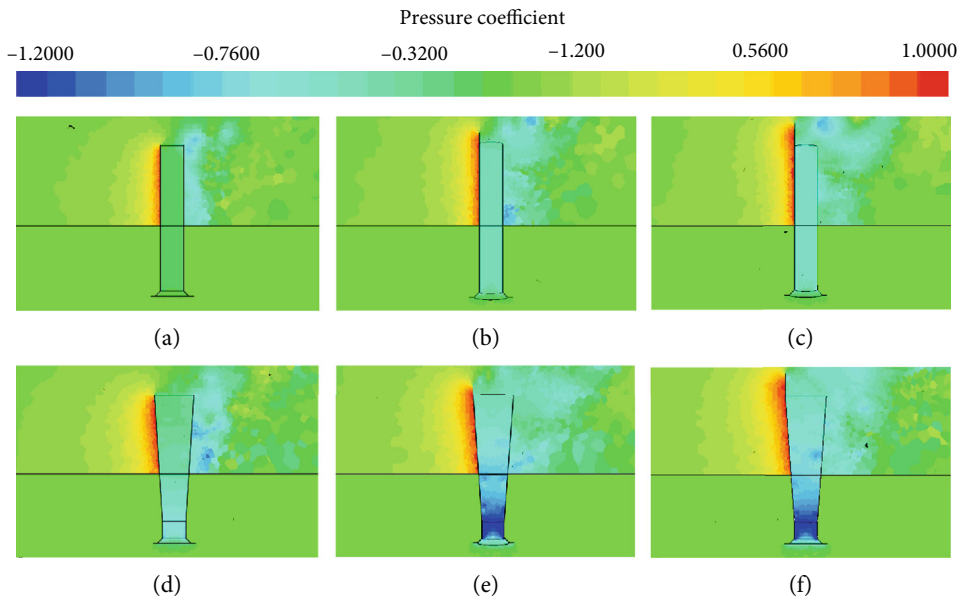

Figure 13: The time-averaged pressure distributions: (a) the cylindrical tower without the vortex generator; (b) the cylindrical tower with the vortex generator ($h_{vg} = D/2$); (c) the cylindrical tower with the vortex generator ($h_{vg} = D$); (d) the diffuser-shaped tower without the vortex generator; (e) the diffuser-shaped tower with the vortex generator ($h_{vg} = D/2$); (f) the diffuser-shaped tower with the vortex generator ($h_{vg} = D$).

Accordingly, pressures inside the towers with the vortex generator were entirely more decreased than towers without the vortex generator. Another notable point was that we captured pressure gradients in the vertical directions inside the towers. The pressures became lower near the bottom of diffuser-shaped towers, although no pressure gradient existed in the cylindrical towers. The pressure gradients corresponded to the flow accelerations by the diffuser effect of the towers. Consequently, the updraft was the most accelerated at the bottom of the diffuser-shaped tower with the vortex generator.

Wind accelerations at the bottom of the towers were preferable because the turbine of the wind solar tower was located

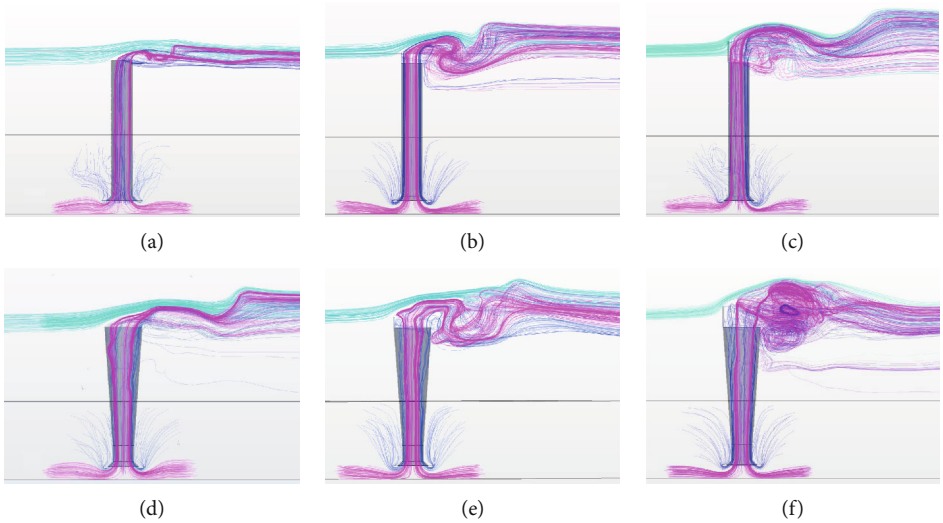

Figure 14: The time-averaged streamlines: (a) the cylindrical tower without the vortex generator; (b) the cylindrical tower with the vortex generator ($h_{vg} = D/2$); (c) the cylindrical tower with the vortex generator ($h_{vg} = D$); (d) the diffuser-shaped tower without the vortex generator; (e) the diffuser-shaped tower with the vortex generator ($h_{vg} = D/2$); (f) the diffuser-shaped tower with the vortex generator ($h_{vg} = D$).

Figure 15: The wind solar tower prototype in Chikushi Campus, Kyushu University.

there. That was, the diffuser-shaped tower with vortex generator was a suitable shape to generate updraft effectively at the desired position.

Figure 14 shows time-averaged streamlines. Large vortices were simulated above the towers which had the vortex generator. The large vortices were also observed in the flow visualizations in the wind tunnel experiments (see Figure 7). The numerical results confirmed that our vortex generators produced vortices adequately near the tower outlets.

3.3. Future Possibilities. Future possibilities of adopting the ideas presented in this paper are worth mentioning. We built a WST prototype in Kyushu University, Japan (see Figure 15). The tower height is 10 m, and the collector width is 15 m. Figure 16 shows the experimental result of remarkable two days. The tower had strong wind in the nighttime. Normally, a solar updraft tower cannot produce updraft after the sunset. However, the WST which utilizes solar energy and wind energy simultaneously was able to generate updraft continually during the nighttime as shown in Figure 16. It meant that we demonstrated the new power generation mechanism of the WST which utilized crosswind

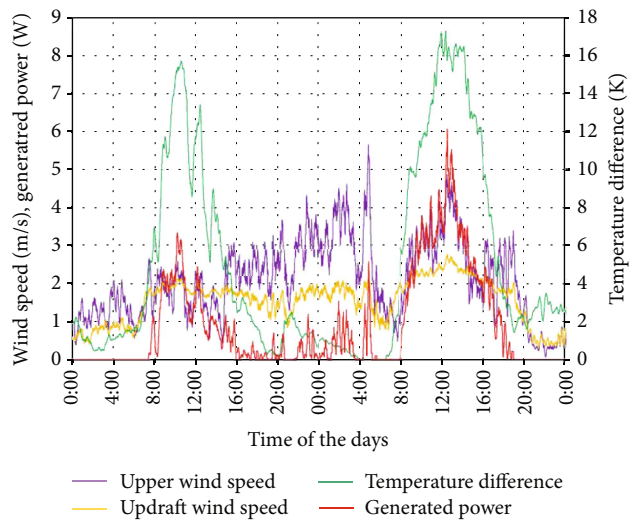

Figure 16: The field experimental results (moving average of the values in every 10 minutes).

energy without solar energy under the practical condition. Unfortunately, the wind speed was not enough to continue the turbine rotation at the nighttime. However, the turbine of the WST in actual size is expected to rotate continually due to its lower cut-in characteristic and its utilization of upper wind without deceleration. Synergy of solar energy and wind energy will be reported with the details of the field test in our future papers.

4. Conclusions

An effective utilization of crosswind energy with a solar updraft tower was investigated using a vortex generator and

a diffuser-shaped tower. The following results were achieved in wind tunnel experiments and numerical simulations.

(i) Suctioned updraft speed in the tower was proportional to the crosswind speed, and its conversion rate depended on the tower configuration

(ii) The diffuser-shaped tower without the vortex generator achieved 2.1 times increase in the updraft speed compared to the cylindrical tower. The diffuser-shaped tower with the vortex generator achieved over 1.3 times increase in the updraft speed

(iii) A diffuser-shaped tower with a vortex generator achieved to produce the updraft whose speed exceeded the crosswind speed. It was due to the low pressure created by the vortex atop the tower and to the diffuser effect

The crosswind utilization enables the simple power generation device to generate electricity during the night, and the hybrid utilization of renewable energies will contribute the increasing wind energy market.

Data Availability

The data used to support the findings of this study are available from the corresponding author upon request.

Conflicts of Interest

The authors declare that there is no conflict of interest regarding the publication of this paper.

Acknowledgments

The authors are grateful to laboratory engineers, Kenichiro Sugitani, Kimihiko Watanabe, and Keiji Matsushima. Advice and comments given by Ai Watanabe were a great help during writing. This research was supported by the grants from Kyushu University.

References

[1] W. Haaf, K. Friedrich, G. Mayr, and J. Schlaich, "Solar chimneys part I: principle and construction of the pilot plant in Manzanares," *International Journal of Solar Energy*, vol. 2, no. 1, pp. 3–20, 1983.

[2] W. Haaf, "Solar Chimneys," *International Journal of Solar Energy*, vol. 2, no. 2, pp. 141–161, 1984.

[3] C. C. Wight, *Wind-driven power generator*, vol. 16, United States patent 4963761, 1990.

[4] E. L. Carson and D. W. Carson, *Whirlwind power system*, vol. 19, United States patent 4018543, 1977.

[5] J. P. Pretorius and D. G. Kröger, "The influence of environment on solar chimney power plant performance," *R & D Journal of the South African Institution of Mechanical Engineering*, vol. 25, 2009.

[6] T. Ming, J. Gui, R. K. de Richter, Y. Pan, and G. Xu, "Numerical analysis on the solar updraft power plant system with a blockage," *Solar Energy*, vol. 98, pp. 58–69, 2013.

[7] T. Ming, Y. Wu, R. K. de_Richter, W. Liu, and S. A. Sherif, "Solar updraft power plant system: a brief review and a case study on a new system with radial partition walls in its collector," *Renewable and Sustainable Energy Reviews*, vol. 69, pp. 472–487, 2017.

[8] Z. Zou, H. Gong, X. Lie, X. Li, and Y. Yang, "Numerical investigation of the crosswind effects on the performance of a hybrid cooling-tower-solar-chimney system," *Applied Thermal Engineering*, vol. 126, pp. 661–669, 2017.

[9] T. Ming, X. Wang, R. K. de Richter, W. Liu, T. Wu, and Y. Pan, "Numerical analysis on the influence of ambient crosswind on the performance of solar updraft power plant system," *Renewable and Sustainable Energy Reviews*, vol. 16, no. 8, pp. 5567–5583, 2012.

[10] W. Shen, T. Ming, Y. Ding, Y. Wu, and R. K. de_Richter, "Numerical analysis on an industrial-scaled solar updraft power plant system with ambient crosswind," *Renewable Energy*, vol. 68, pp. 662–676, 2014.

[11] J. O. C. Silva, L. P. Gonçalves, L. F. R. Ledo, C. B. Maia, S. M. Hanriot, and J. Landre, "Numerical analysis of the crosswind in small solar chimney," in *proceedings of the 12th international conference on heat transfer, fluid mechanics and thermodynamics*, Malaga, Spain, July 2016.

[12] J. O. C. Silva, D. S. S. Machado, J. A. D. Silva, and C. B. Maia, "Numerical determination of the coefficient of heat transfer by convection between coverage and external environment in a small solar chimney," in *proceedings of the 24th ABCM international congress of mechanical engineering*, Curitiba, Brazil, December 2017.

[13] N. Jafarifar, M. M. Behzadi, and M. Yaghini, "The effect of strong ambient winds on the efficiency of solar updraft power towers: a numerical case study for Orkney," *Renewable Energy*, vol. 136, pp. 937–944, 2019.

[14] Y. Ohya, M. Wataka, K. Watanabe, and T. Uchida, "Laboratory experiment and numerical analysis of a new type of solar tower efficiently generating a thermal updraft," *Energies*, vol. 9, no. 12, p. 1077, 2016.

[15] Y. Ohya and T. Karasudani, "A shrouded wind turbine generating high output power with wind-lens technology," *Energies*, vol. 3, no. 4, pp. 634–649, 2010.

[16] K. Watanabe and Y. Ohya, "Multi-rotor systems using three shrouded wind turbines for power output increase," *Journal of Energy Resources Technology*, vol. 141, no. 5, 2019.

[17] K. Watanabe, Y. Ohya, and T. Uchida, "Power output enhancement of a ducted wind turbine by stabilizing vortices around the duct," *Energies*, vol. 12, no. 16, p. 3171, 2019.

[18] T. T. Chow, G. N. Tiwari, and C. Menezo, "Hybrid solar: a review on photovoltaic and thermal power integration," *International Journal of Photoenergy*, vol. 2012, Article ID 307287, 17 pages, 2012.

[19] Q. Liu, F. Cao, Y. Liu, T. Zhu, and D. Liu, "Design and simulation of a solar chimney PV/T power plant in northwest China," *International Journal of Photoenergy*, vol. 2018, Article ID 1478695, 12 pages, 2018.

[20] "Siemens Product Lifecycle Management Software Inc.," October 2019 https://www.plm.automation.siemens.com/global/en/products/simcenter/STAR-CCM.html.